Cancer Cell
Article

Cancer Metastasis Is Accelerated through Immunosuppression during Snail-Induced EMT of Cancer Cells

Chie Kudo-Saito,[1,*] Hiromi Shirako,[1] Tadashi Takeuchi,[1] and Yutaka Kawakami[1,*]
[1]Division of Cellular Signaling, Institute for Advanced Medical Research, Keio University School of Medicine, Tokyo 160-8582, Japan
*Correspondence: kudoc@sc.itc.keio.ac.jp (C.K.-S.), yutakawa@sc.itc.keio.ac.jp (Y.K.)
DOI 10.1016/j.ccr.2009.01.023

SUMMARY

Epithelial-mesenchymal transition (EMT) is a key step toward cancer metastasis, and Snail is a major transcription factor governing EMT. Here, we demonstrate that Snail-induced EMT accelerates cancer metastasis through not only enhanced invasion but also induction of immunosuppression. Murine and human melanoma cells with typical EMT features after *snail* transduction induced regulatory T cells and impaired dendritic cells in vitro and in vivo partly through TSP1 production. Although Snail$^+$ melanoma did not respond to immunotherapy, intratumoral injection with *snail*-specific siRNA or anti-TSP1 monoclonal antibody significantly inhibited tumor growth and metastasis following increase of tumor-specific tumor-infiltrating lymphocytes and systemic immune responses. These results suggest that inhibition of Snail-induced EMT could simultaneously suppress both tumor metastasis and immunosuppression in cancer patients.

INTRODUCTION

Epithelial-mesenchymal transition (EMT) is a transdifferentiation characterized by decreased epithelial markers such as E-cadherin and increased mesenchymal markers such as fibronectin (Hay, 1995; Radisky, 2005). It is a dynamic process to acquire cell motility with decreased adhesive ability for body organization, including embryonic development and wound healing. Currently, EMT is thought to be a key step for cancer metastasis (Hugo et al., 2007; Radisky, 2005). Many EMT inducers such as TGF-β (Peinado et al., 2003) and VEGF (Yang et al., 2006) have been identified, and the molecular mechanisms related to the highly invasive characteristics of cancer cells have been intensively investigated (Huber et al., 2005; Radisky, 2005). Snail is a major transcription factor frequently upregulated by various EMT inducers in a variety of cancers, while EMT is regulated by many transcription factors such as Slug and Twist. However, the interaction between cancer cells and host immunity during EMT has not yet been evaluated. In this study, we investigated the significance of Snail-induced EMT for antitumor immune responses in hosts with progressive cancers.

RESULTS

Establishment of Murine Melanoma Cell Lines with EMT-like Features by *snail* Transduction

To evaluate interaction between immune cells and tumor cells during EMT, we first established murine melanoma B16-F10 cells with EMT-like features after transduction with murine *snail* cDNA using electroporation. Snail is one of the major transcription factors governing EMT of various cancer cells, and its increase in tumor tissues of patients is correlated with tumor progression (metastasis and recurrence) in various cancers including melanoma (Dissanayake et al., 2007; Kuphal et al., 2005; Moody et al., 2005), hepatocellular carcinoma (Sugimachi et al., 2003), head and neck squamous cell carcinoma (Yang et al., 2007), and endometrial cancers (Becker et al.,

SIGNIFICANCE

Epithelial-mesenchymal transition (EMT) is considered to be an important step for cancer cells to metastasize. Its molecular mechanisms have been intensively elucidated from aspects of cancer invasion, and Snail is thought to be a major transcription factor frequently involved in EMT in various cancers. Here, we demonstrate that Snail-induced EMT accelerates cancer metastasis utilizing not only the enhanced invasive ability but also induction of multiple immunosuppression and immunoresistance mechanisms including immunosuppressive cytokines, regulatory T cells, impaired dendritic cells, and cytotoxic T lymphocyte resistance. Snail blockade simultaneously inhibits both cancer invasion and the multiple immunosuppressions, resulting in efficient inhibition of cancer metastasis. This strategy targeting EMT-regulating Snail may be useful for cancer treatments, especially for immunotherapy, which should restore immunocompetence in patients.

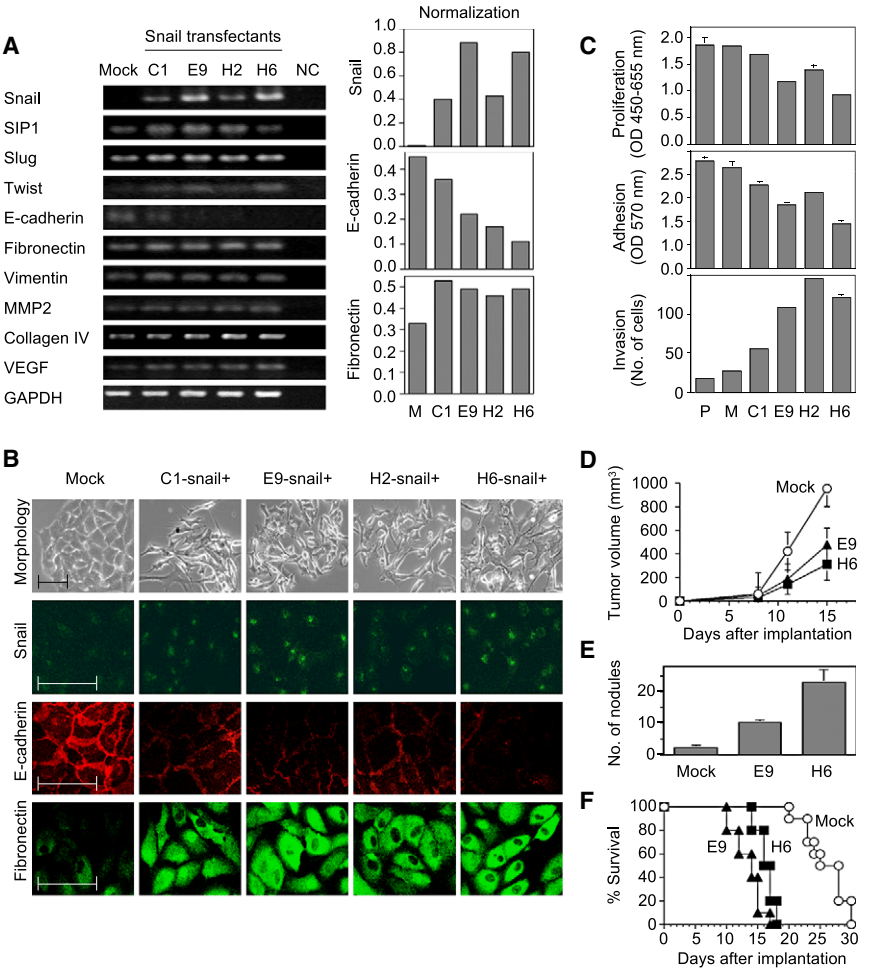

Figure 1. *snail*-Transduced Murine Melanoma B16-F10 Cells with EMT-like Characteristics

(A) Left: decrease of epithelial markers and increase of mesenchymal markers in Snail transfectants detected by RT-PCR. Right: the intensity of *snail*, *E-cadherin*, and *fibronectin* was normalized to *GAPDH* expression as a control.

(B) Decreased E-cadherin and increased fibronectin in the Snail transfectants with spindle and dendritic shapes (immunocytochemistry; scale bars = 0.5 mm).

(C) Decreased proliferation and adhesion and increased invasion of Snail transfectants (n = 3, mean ± SD).

(D) Suppressed growth of Snail transfectants in vivo. C57BL/6 mice were implanted subcutaneously (s.c.) with tumor cells (n = 5, mean ± SD).

(E) Enhanced in vivo metastatic ability of Snail transfectants. Mice were implanted intravenously (i.v.) with tumor cells, and the numbers of nodules in lungs of the mice were counted on day 14 after tumor implantation (n = 5, mean ± SD).

(F) Decreased survival of mice with Snail transfectants. Mice were implanted i.v. with tumor cells.

Data shown in each panel are representative of four independent experiments.

2007). It has been reported in melanoma that downregulation of E-cadherin caused by Snail disrupts growth control by keratinocytes and leads to melanoma progression (Herlyn et al., 2000). After G418 selection, four clones were evaluated for EMT characteristics. Although *snail* was slightly expressed in the parental B16-F10 cells or B16-F10 cells mock-transfected with empty vector, *snail* expression was markedly increased in these Snail transfectants (Figures 1A and 1B). Along with the *snail* increase, these clones showed EMT-like changes in mRNA (Figure 1A) and protein expression (Figure 1B) and cellular characteristics (Figure 1C) such as decreased E-cadherin (an epithelial maker) and increased fibronectin (a mesenchymal marker), spindle and dendritic shapes, decreased cell proliferation, decreased cell adhesion, and increased cell invasion as compared with the parental B16-F10 cells or mock transfectants. Two Snail transfectants, E9-snail+ and H6-snail+ tumor cells, were selected for further studies due to having the typical EMT-like characteristics. When these Snail transfectants were implanted subcutaneously (s.c.) or intravenously (i.v.) into C57BL/6 mice, the s.c. tumors grew slowly (Figure 1D), more tumor cells metastasized to the lungs (Figure 1E), and these mice showed decreased survival (Figure 1F) as compared to mock tumor-implanted mice (significant difference, $p < 0.01$).

Induction of Immunosuppressive CD4$^+$Foxp3$^+$ Cells by *snail*-Transduced Melanoma Cells

Using these Snail transfectants with EMT-like characteristics, we examined how EMT would influence immune responses. When spleen cells (SPCs) were cultured with Snail$^+$ tumor cells for 5 days, SPC proliferation was decreased ($p < 0.03$; Figure 2A), and both CD4$^+$ and CD8$^+$ cells were decreased in the culture (Figure 2B) as compared to SPCs cultured with Snail$^-$ parental or mock-transfected tumor cells. Although CD4$^+$CD25$^+$ cells including immunosuppressive naturally occurring regulatory T (nTreg) cells were not increased in the culture, Foxp3, a master transcription factor for immunosuppressive function of nTreg cells, was significantly induced in the CD4$^+$CD25$^-$ cells as compared with those cultured with Snail$^-$ tumor cells ($p < 0.017$; Figure 2C; see also Table S1 available online). Other molecules such as CTLA-4, HO-1, granzyme B, and PD-1 expressed in CD4$^+$CD25$^+$ nTreg cells were also expressed in the H6-stimulated CD4$^+$ cells as well as nTreg cells (Figure S1). To determine whether these immunosuppressive cascades were caused by Snail expression, siRNAs specific for murine *snail* were transfected into the H6-snail+ tumor cells. Along with downregulation of *snail* expression, cell invasion and the ability to induce CD4$^+$Foxp3$^+$ cells were significantly decreased in H6-snail+ tumor cells by *snail*-specific siRNA transfection as compared with cells transfected with the scramble oligonucleotide control (Figures S2A–S2D). The *snail*-specific siRNA #2 was also effective in suppressing *snail* expression in H6-snail+ tumors implanted s.c. into mice by intratumoral injection (Figure S2E). These data confirm the essential role of *snail* in tumor cells for Treg-like CD4$^+$Foxp3$^+$

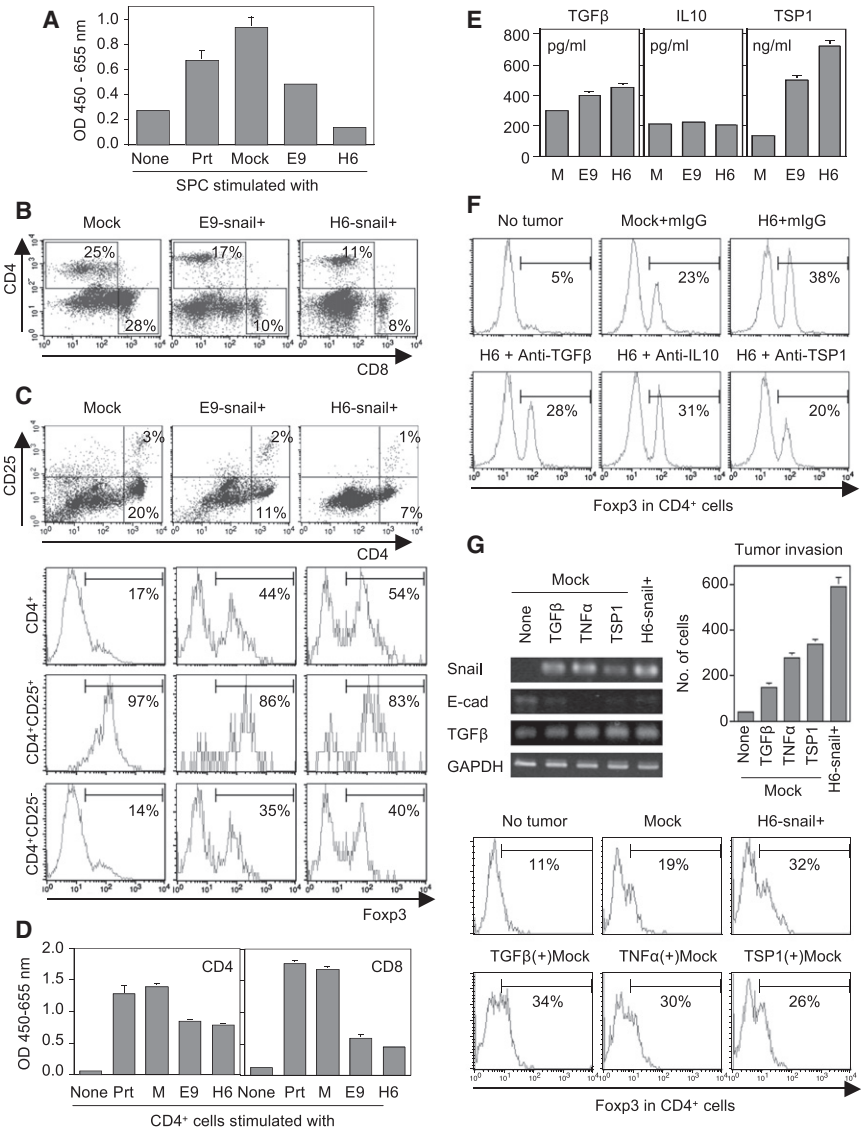

Figure 2. Induction of Immunosuppressive CD4$^+$Foxp3$^+$ Cells by Snail$^+$ Tumor Cells

(A) Inhibition of splenic cell proliferation by Snail transfectants. Spleen cells (SPCs) were cocultured with tumor cells for 5 days (n = 3, mean ± SD).

(B) Inhibition of T cell induction in the SPC culture by Snail transfectants. The percentage of CD4$^+$ or CD8$^+$ cells was analyzed by flow cytometry.

(C) Foxp3 induction in the CD4$^+$ cells of SPCs by coculture with Snail transfectants. The percentage of Foxp3$^+$ cells was analyzed after gating CD4$^+$ cells (upper row), CD4$^+$CD25$^+$ cells (middle row), or CD4$^+$CD25$^-$ cells (lower row) by flow cytometry.

(D) Immunosuppressive activity of the CD4$^+$ cells stimulated with Snail transfectants. Bulk SPCs were cocultured with tumor cells for 5 days, and CD4$^+$ cells purified from the culture were tested for immunosuppressive activity on T cell proliferation in response to anti-CD3 monoclonal antibody (mAb) (n = 3, mean ± SD).

(E) Production of regulatory T (Treg)-inducible cytokines from Snail transfectants. Tumor supernatants cultured for 3 days were tested for each cytokine using ELISA (n = 3, mean ± SD).

(F) Suppression of Foxp3 induction in CD4$^+$ cells by mAb addition to Snail transfectants. The percentage of Foxp3$^+$ cells was analyzed after gating CD4$^+$ cells by flow cytometry.

(G) Foxp3 induction in CD4$^+$ cells cocultured with B16-F10 tumor cells with increased Snail along with high invasive ability after cytokine treatment (tumor invasion: n = 3, mean ± SD). mRNA expression of *snail*, *E-cadherin*, and *TGF-β* was detected by RT-PCR. The percentage of Foxp3$^+$ cells was analyzed after gating CD4$^+$ cells by flow cytometry. Data shown in each panel are representative of three independent experiments.

cell induction as well as cell motility. To evaluate suppressive activity of the CD4$^+$ cells cocultured with tumor cells, CD4$^+$ cells were separated from the culture and added to a T cell proliferation assay, where fresh splenic CD4$^+$ or CD8$^+$ cells were stimulated with anti-CD3 monoclonal antibody (mAb) and irradiated SPCs as antigen-presenting cells (APCs) for 5 days. The CD4$^+$ cells precultured with H6-snail+ tumor cells significantly suppressed proliferation of T cells, particularly CD8$^+$ T cells, as compared with the CD4$^+$ cells precultured with Snail$^-$ tumor cells ($p < 0.001$; Figure 2D). The induction of such immunosuppressive CD4$^+$Foxp3$^+$ cells was also observed when SPCs were cultured with the other Snail transfectants or the culture supernatants, although their efficacies were lower than those of E9-snail+ and H6-snail+ tumor cells having higher Snail expression (data not shown). These results indicate that Snail$^+$ B16-F10 cells in EMT generate immunosuppressive CD4$^+$Foxp3$^+$ cells.

TGF-β, IL-10, and thrombospondin-1 (TSP1) have been reported to induce Treg cells (Futagami et al., 2007; von Boehmer, 2005; Crawford et al., 1998). We examined whether these cytokines would be involved in the CD4$^+$Foxp3$^+$ cell induction by Snail$^+$ melanoma. Production of TGF-β and TSP1, but not IL-10, was significantly greater in Snail$^+$ melanoma cells than in Snail$^-$ melanoma cells ($p < 0.05$; Figure 2E). The specific mAbs, particularly anti-TSP1 mAb, markedly inhibited Foxp3 induction in CD4$^+$ cells of SPCs cocultured with H6-snail+ tumor cells (Figure 2F). Anti-TSP1 mAb was also effective in suppressing CD4$^+$Foxp3$^+$ Treg induction caused by the parental B16-F10 melanoma (Foxp3$^+$ cells in the CD4$^+$ cells cocultured with mock transfectant: 23% for mIgG versus 15% for anti-TSP1 mAb). The inhibitory efficacy of the anti-TSP1 mAb on the H6-induced Treg generation was statistically significant compared to that of the control mIgG ($p < 0.047$; Table S1). These results indicate that TSP1 is a potent mediator involved in the Treg induction caused by Snail$^+$ melanoma cells.

We further examined whether tumor cells with increased Snail during naturally occurring EMT would induce Treg cells. When B16-F10 (mock tumor) cells were treated with TGF-β or TNFα for 3 days, expression of both *snail* and *TGF-β* was enhanced in the tumor cells, along with reduced *E-cadherin* and augmented invasive ability (Figure 2G). Foxp3 was increased in CD4$^+$ cells when cocultured with these tumor cells for 5 days (Figure 2G).

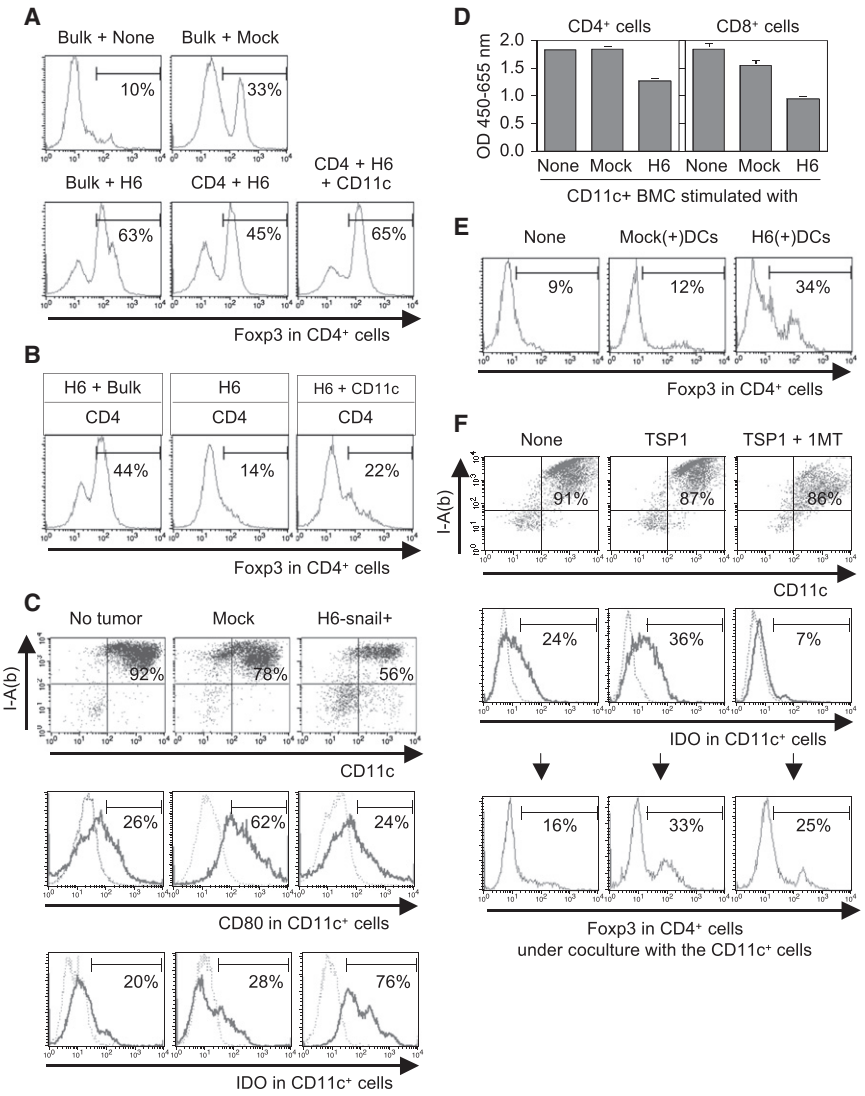

Figure 3. Involvement of Immunosuppressive CD11c$^+$ Cells in CD4$^+$Foxp3$^+$ Cell Induction

(A) Enhancement of Foxp3 induction in CD4$^+$ cells cocultured with H6-snail+ tumor cells in the presence of CD11c$^+$ cells.

(B) Requirement of cell-cell contact among CD4$^+$ cells, H6-snail+ tumor cells, and CD11c$^+$ cells for Treg induction. CD4$^+$ cells were separately cultured with H6-snail+ tumor cells or CD11c$^+$ cells using transwell chambers.

(C) Generation of CD11c$^+$I-A^{b+} cells with low CD80 and high IDO expression by coculture with H6-snail+ tumor cells.

(D) Immunosuppressive activity of H6-stimulated CD11c$^+$ cells on T cell proliferation. CD11c$^+$ cells from bone marrow were stimulated with granulocyte macrophage colony-stimulating factor (GM-CSF) and tumor cells for 6 days, and these cells were added to fresh CD4$^+$ or CD8$^+$ T cells with anti-CD3 mAb (n = 3, mean ± SD).

(E) Foxp3 induction in CD4$^+$ cells by coculture with H6-prestimulated CD11c$^+$ cells. The percentage of Foxp3$^+$ cells was analyzed after gating CD4$^+$ cells by flow cytometry.

(F) Generation of Treg-inducible CD11c$^+$ cells by TSP1 stimulation. CD11c$^+$ cells from bone marrow were stimulated with TSP1 with or without the IDO inhibitor 1-methyltryptophan (1MT) in addition to GM-CSF for 6 days and were analyzed for IDO expression by flow cytometry. Fresh CD4$^+$ T cells were cocultured with these CD11c$^+$ cells with anti-CD3 mAb and analyzed for Foxp3 expression after gating CD4$^+$ cells by flow cytometry.

Data shown in each panel are representative of two independent experiments.

Interestingly, TSP1 similarly caused these phenomena, indicating that TSP1 could be also an EMT inducer, perhaps by mediating through TGF-β induction and activation as reported. These results suggest that Treg cells can be induced by Snail$^+$ tumors during naturally occurring EMT in melanoma. TGF-β and TSP1 from such tumors could be partly responsible for both Treg induction and the further enhancement of EMT in an autocrine manner.

Treg Induction Mediated by Immunosuppressive CD11c$^+$ Dendritic Cells Generated by Snail$^+$ Melanoma Cells

We next examined whether CD4$^+$Foxp3$^+$ Treg cells would be induced directly by Snail$^+$ melanoma cells or indirectly via other immune cells such as APCs. Foxp3 was increased in purified CD4$^+$ T cells by coculture with H6-snail+ tumor cells and was augmented by addition of purified CD11c$^+$ splenic cells (Figure 3A, lower panels). However, the effect was reduced when CD4$^+$ cells were separately cultured with CD11c$^+$ cells using transwell chambers, indicating requirement of cell-cell contact among CD4$^+$ cells, CD11c$^+$ cells, and Snail$^+$ tumor cells for optimal Treg induction (Figure 3B). These results indicate that CD11c$^+$ cells mediate Treg induction by Snail$^+$ melanoma cells.

We further examined the effects of Snail$^+$ melanoma cells on CD11c$^+$ cells. CD11c$^+$ cells enriched from bone marrow cells (BMCs) were cultured with tumor cells in the presence of granulocyte macrophage colony-stimulating factor (GM-CSF) for 6 days. When CD11c$^+$ BMCs were cultured with Snail$^-$ melanoma cells, almost all of the cells were differentiated into mature dendritic cells (DCs) with high expression of I-A^b and CD80 (Figure 3C). These cells induced proliferation of both CD4$^+$ and CD8$^+$ splenic T cells (Figure 3D). In contrast, when cultured with H6-snail+ tumor cells, CD11c$^+$ BMCs were differentiated into possibly regulatory DCs with low expression of I-A^b and CD80 and high expression of the immunosuppressive enzyme indoleamine 2,3-dioxygenase (IDO) (Figure 3C). The T cell proliferative activity of these DCs was significantly less than that of DCs cultured with mock transfectant ($p < 0.03$; Figure 3D). In addition, Foxp3 increase was observed in the CD4$^+$ cells stimulated with the H6(+) CD11c$^+$ BMCs (Figure 3E). These results indicate that Treg cells are induced partly by impaired DCs generated by Snail$^+$ tumor cells.

TSP1 is also known to be a negative regulator of DC functions (Doyen et al., 2003). We examined whether TSP1 would be involved in the DC impairment induced by Snail$^+$ tumor cells

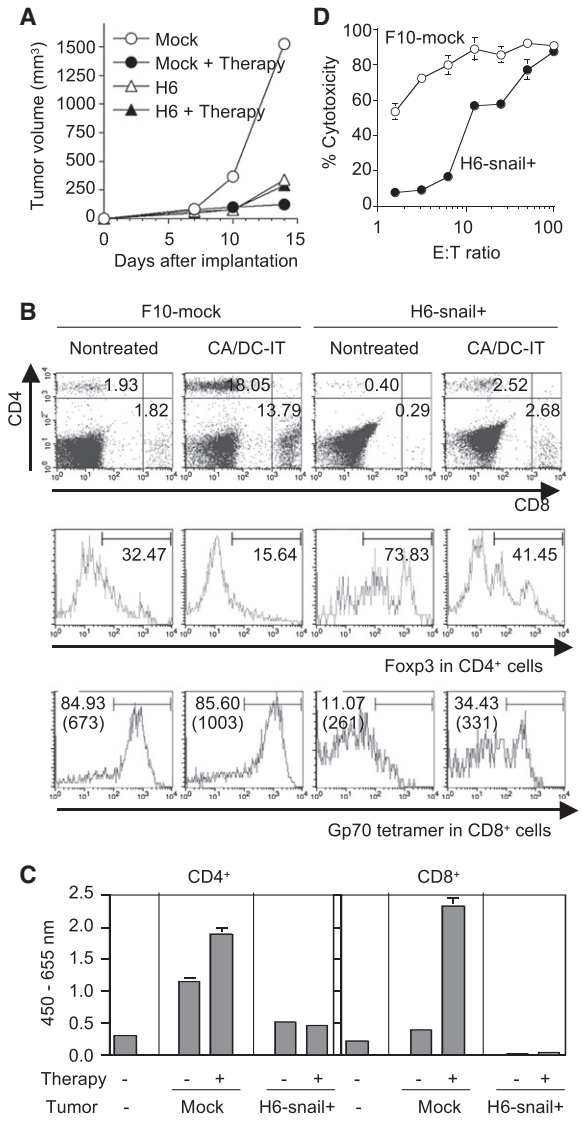

Figure 4. Resistance of Snail⁺ Melanoma to Immunotherapy

(A) H6-snail+ melanoma growth is not inhibited by immunotherapy with cryoablation of tumors followed by intratumoral (i.t.) injection of gp70 peptide-pulsed dendritic cells (DCs) (CA/DC-IT; n = 5–7, mean).

(B) No increase in infiltration of gp70 tetramer-binding CD8⁺ T cells was detected in H6-snail+ tumor tissues on day 7 after the therapy. The percentage of each positive fraction was analyzed by flow cytometry. The numbers in parentheses indicate the gp70 tetramer mean fluorescence intensity (MFI) of gp70 tetramer-binding CD8⁺ cells.

(C) No proliferation of splenic T cells from mice with H6-snail+ tumors is observed even after CA/DC-IT therapy. CD4⁺ or CD8⁺ cells purified from SPCs of these mice were stimulated with anti-CD3 mAb and antigen-presenting cells (APCs) for 5 days (n = 3, mean ± SD).

(D) Resistance of H6-snail+ tumor cells to killing by gp70-specific cytotoxic T lymphocytes (CTLs) (n = 3, mean ± SD). CTLs were induced using SPCs from F10-mock(+) mice receiving CA/DC-IT therapy. White circles indicate % specific lysis of mock-transfected tumor cells. Black circles indicate % specific lysis of H6-snail+ cells.

Data shown in each panel are representative of two independent experiments.

as well as Treg induction. TSP1-pretreated CD11c⁺ cells increased Foxp3 in CD4⁺ cells when cocultured (Figure 3F). When mAbs specific for TSP1 or TSP1 receptors (CD36 or CD47) expressed on DCs were added to the CD11c⁺ cell culture with TSP1, Treg induction was decreased (Figure S3A), suggesting that Treg induction could be partly mediated by immunosuppressive DCs generated by TSP1 from Snail⁺ tumor cells. In the TSP1-treated CD11c⁺ cells, however, IDO expression was enhanced only slightly. Also, Treg induction was not completely inhibited despite almost complete absence of IDO expression in CD11c⁺ cells treated with the IDO inhibitor 1-methyltryptophan (1MT). These results suggest that IDO is not significantly involved in the Treg induction by TSP1-treated CD11c⁺ cells.

Resistance of Snail⁺ Melanoma to Immunotherapy

Next, the susceptibility of Snail⁺ melanoma to immunotherapy was evaluated. H6-snail+ tumor cells implanted s.c. into C57BL/6 mice grew significantly less than the mock-transfected tumor cells ($p < 0.001$; Figure 4A). Immunotherapy with cryoablation of tumors followed by intratumoral (i.t.) injection of DCs pulsed with tumor antigen gp70/H-2K^b peptide (CA/DC-IT) significantly inhibited growth of mock-transfected tumors, but not H6-snail+ tumors in spite of their slower growth ($p < 0.0001$; Figure 4A). Although mock-transfected tumors disappeared in 4–5 of 7 mice treated, H6-snail+ tumors showed no regression in the mice treated. The CA/DC-IT therapy greatly increased infiltration of both gp70 tetramer-binding CD8⁺ cells and CD4⁺ cells with low Foxp3 expression in mock-transfected tumor tissues (Figure 4B) and also systemically in the regional lymph nodes, spleens, and peripheral blood of the mice (Table S2). However, only a small increase of T cell infiltration including CD8⁺ cells with much lower gp70 tetramer binding and CD4⁺ cells with higher Foxp3 expression was observed in H6-snail+ tumors treated with the therapy (Figure 4B). It should be noted that after the CA/DC-IT therapy, the mean fluorescence intensity (MFI) of gp70 tetramer binding was also increased in the CD8⁺ cells of F10-mock(+) mice (from 673 to 1003), while remaining low in the CD8⁺ cells of H6(+) mice (from 261 to 331), indicating almost no induction of tumor-specific CD8⁺ cells with high T cell receptor avidity. In the H6(+) mice receiving the therapy, CD4⁺Foxp3⁺ cells were decreased in the regional lymph nodes, but not in spleens and peripheral blood, and no increase of gp70 tetramer-binding CD8⁺ cells was observed systemically in these peripheral tissues (Table S2). When splenic T cells from these mice were stimulated with anti-CD3 mAb and APCs in vitro for 5 days, the proliferative ability of both CD4⁺ and CD8⁺ cells was significantly augmented in F10-mock(+) mice after CA/DC-IT therapy ($p < 0.01$; Figure 4C). However, splenic T cells from H6(+) mice did not proliferate even after the therapy. Interestingly, H6-snail+ tumor cells were resistant to cytolysis by gp70-specific cytotoxic T lymphocytes (CTLs), which demonstrated higher cytotoxicity to mock tumor cells (Figure 4D). These results indicate that Snail⁺ melanoma cells are resistant to immunotherapy due to both inhibition of antitumor immune induction via immunosuppression and decreased sensitivity to CTL lysis.

To clarify the relationship between tumors with Snail increased by naturally occurring EMT and immunoresistance, we further conducted the same CA/DC-IT therapy using mice implanted with B16-F10 tumor cells with high Snail expression

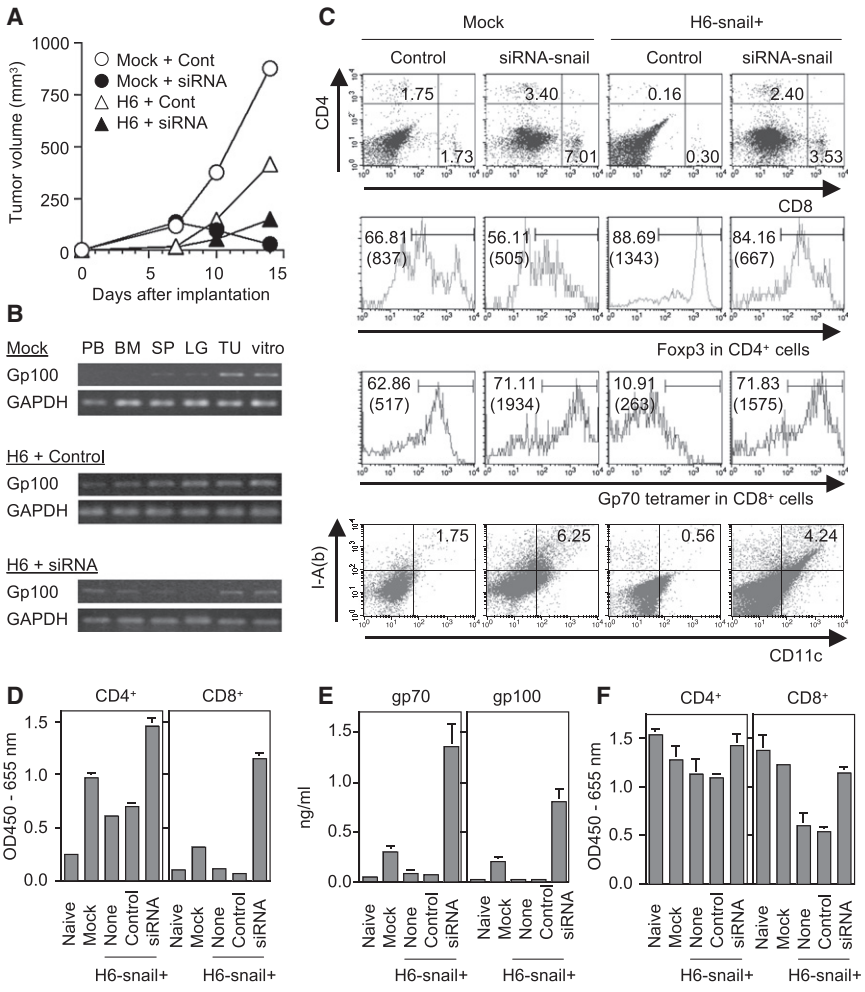

Figure 5. Abrogation of Snail$^+$ Tumor-Induced Immunosuppression In Vivo by Intratumoral Injection with *snail*-Specific siRNA

(A) Inhibition of H6-snail+ tumor growth by *snail*-specific siRNA injection. C57BL/6 mice received i.t. injection with PEI-complexed *snail*-specific siRNA #2 or scrambled oligonucleotide control on day 7 after tumor implantation and were sacrificed for assays on day 14 (n = 3–5, mean).

(B) Inhibition of systemic micrometastasis of H6-snail+ tumor cells by siRNA-*snail*. Melanoma antigen *gp100* mRNA was detected by RT-PCR. PB, peripheral blood; BM, bone marrow; SP, spleen; LG, lung; TU, tumors subcutaneously implanted; vitro, either mock or H6-snail+ tumor cells cultured in vitro as a control for gp100.

(C) Increased infiltration of CD4$^+$ cells, CD8$^+$ cells, and CD11c$^+$I-A^{b+} cells in tumor tissues injected with siRNA-*snail*. The percentage of each positive fraction was analyzed by flow cytometry. The numbers in parentheses indicate the Foxp3 MFI of CD4$^+$Foxp3$^+$ cells (upper histograms) or the gp70 tetramer MFI of gp70 tetramer-binding CD8$^+$ cells (lower histograms). To analyze T cells infiltrating into H6-snail+ tumors, 1 × 10^4 CD3$^+$ cells were acquired to analyze Foxp3$^+$ expression in CD4$^+$ cells or gp70 tetramer-binding CD8$^+$ cells because these contain very few CD3$^+$ cells in the tumor-infiltrating lymphocytes.

(D) Augmentation of splenic T cell proliferation by siRNA-*snail* injection (n = 3, mean ± SD).

(E) Enhancement of IFN-γ production from splenic CD8$^+$ cells specific for melanoma antigen gp70 and gp100 by siRNA-*snail* injection (n = 3, mean ± SD).

(F) Restoration of APC activity of bone marrow-derived CD11c$^+$ cells on splenic T cell proliferation by siRNA-*snail* injection (n = 3, mean ± SD).

Data shown in each panel are representative of three independent experiments.

and high invasive ability after treatment with TGF-β for 3 days as shown in Figure 2G. When TGF-β-treated tumor cells as well as Snail transfectants were implanted both s.c. and i.v. in C57BL/6 mice, the growth was slower (Figure S4A), metastasis to lungs was increased (Figure S4B), and tumor-infiltrating cells were less numerous (Figure S4C) compared to those of TGF-β(−) tumors (significant difference, $p < 0.0001$). When the TGF-β(+) tumors were treated with the CA/DC-IT therapy on day 5 after tumor implantation, the therapeutic effect was apparently less than on the TGF-β(−) tumors, although showing a significant tumor-suppressive effect on day 14 ($p < 0.0003$; Figures S4A–S4B). The pattern of T cell infiltration into the treated TGF-β(+) tumors was similar to the case of H6-snail+ tumors, in which T cells were only slightly increased by the therapy (Figure S4C). These results indicate that naturally occurring EMT is also associated with resistance to immunotherapy.

Induction of Antitumor Immune Responses by Targeting *snail*

We then attempted to abrogate the immunosuppression by targeting *snail*. Although H6-snail$^+$ tumors grew significantly less than the mock-transfected tumors ($p < 0.001$; Figure 5A), as was the case in vitro (Figure 1C), *gp100*, representative of micrometastasis of the B16-F10 tumor cells, was detected in various organs including peripheral blood, bone marrow, spleens, and lungs of the mice on day 14 (Figure 5B, middle panel), while being only faintly detected in spleens and lungs of mice with mock-transfected tumors (Figure 5B, upper panel), indicating more spontaneously metastatic ability of the Snail$^+$ tumors even by s.c. implantation. When polyethyleneimine (PEI)-complexed siRNA specific for murine *snail* was injected i.t. into H6-snail+ tumors on day 7, tumor growth was significantly inhibited as compared with control scrambled siRNA ($p < 0.001$; Figure 5A), as well as tumor metastasis (Figure 5B, lower panel). Survival of mice was significantly prolonged by the siRNA-*snail* injection when observed over a longer term ($p < 0.008$; mean survival: 15 days for control mice versus 35 days for siRNA-*snail* mice). In the H6-snail+ tumors treated with *snail*-specific siRNA, infiltration of immune cells such as CD4$^+$, CD8$^+$, and CD11c$^+$ cells was markedly increased as compared to that in the control H6-snail+ tumors (Figure 5C). Foxp3 was reduced in the CD4$^+$ cells, gp70 tetramer binding was increased in the CD8$^+$ cells, and I-A^b was enhanced in the CD11c$^+$ cells. As compared with F10-mock(+) mice, splenic

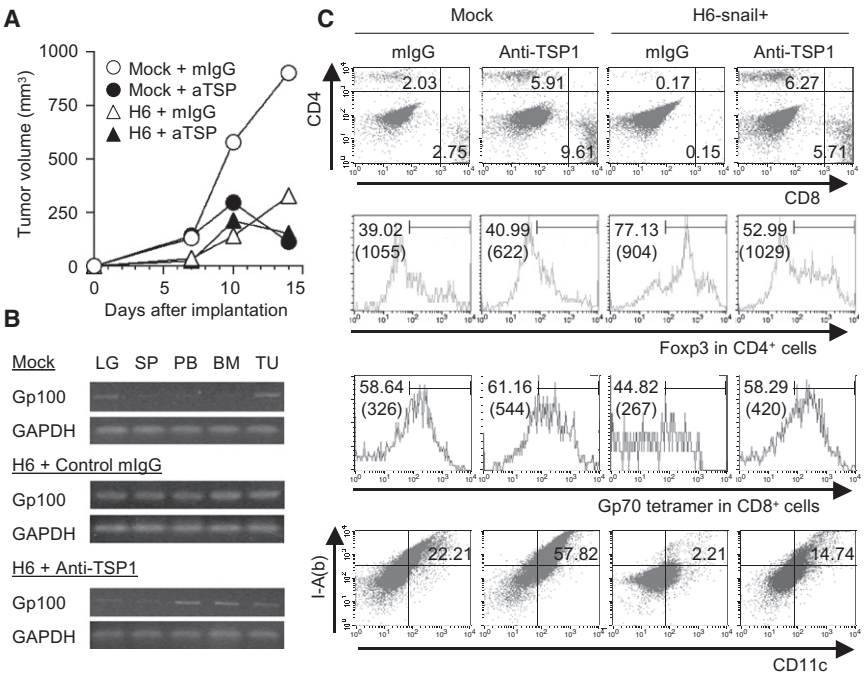

Figure 6. Restoration of Antitumor Effector Cells in Snail⁺ Tumors Injected with Anti-TSP1 Monoclonal Antibody

(A) Inhibition of H6-snail+ tumor growth by anti-TSP1 mAb injection. C57BL/6 mice received intratumoral injection with anti-TSP1 mAb or isotype control mIgG on day 7 after tumor implantation and were sacrificed for assays on day 14 (n = 3, mean).

(B) Inhibition of systemic micrometastasis of H6-snail+ tumor cells by siRNA-*snail*. Melanoma antigen *gp100* mRNA was detected by RT-PCR. LG, lung; SP, spleen; PB, peripheral blood; BM, bone marrow; TU, tumors subcutaneously implanted.

(C) Increased infiltration of CD4⁺ cells, CD8⁺ cells, and CD11c⁺I-A^{b+} cells in tumor tissues injected with anti-TSP1 mAb. The percentage of each positive fraction was analyzed by flow cytometry. The numbers in parentheses indicate the Foxp3 MFI of CD4⁺Foxp3⁺ cells (upper histograms) or the gp70 tetramer MFI of gp70 tetramer-binding CD8⁺ cells (lower histograms).

Data shown in each panel are representative of two independent experiments.

T cells proliferated significantly less ($p < 0.003$; Figure 5D), CD8⁺ T cells produced less IFN-γ in response to the tumor antigen peptides gp70 and gp100 ($p < 0.01$; Figure 5E), and CD11c⁺ BMCs induced less T cell proliferation ($p < 0.001$; Figure 5F) in the H6(+) mice. CD8⁺ T cell responses were particularly impaired in the H6(+) mice. However, all of these antitumor immune responses were restored by i.t. injection of siRNA-*snail* into H6-snail+ tumors ($p < 0.001$; Figures 5D–5F). These results indicate that Snail⁺ melanoma cells induce in vivo immunosuppression through induction of CD4⁺Foxp3⁺ Treg cells and impaired DCs as observed in vitro. Such immunosuppression could inhibit induction of antitumor immune responses and accelerate tumor metastasis. This suggests that *snail*-targeting therapy could augment antitumor immune responses by abrogating tumor-induced immunosuppression.

TSP1 Is Involved in Snail-Induced Immunosuppression

We next attempted to determine the mechanisms for the Snail-induced immunosuppression in vivo by focusing on TSP1, because TSP1 was most significantly increased in *snail*-transduced B16-F10 melanoma (Figure 2E) and because anti-TSP1 mAb most strongly inhibited CD4⁺Foxp3⁺ Treg induction by the Snail transfectants as compared with other Treg-inducible cytokines (Figure 2F). H6-snail⁺ tumor growth and metastasis were significantly inhibited by i.t. injection with anti-TSP1 mAb on day 7 as compared with mice injected with the isotype control ($p < 0.03$; Figures 6A and 6B). Survival was significantly prolonged by the anti-TSP1 mAb injection when observed over a longer term ($p < 0.0001$; 16 days for mIgG(+) mice versus 28 days for anti-TSP1 mAb(+) mice). When anti-TGF-β mAb was injected, since TSP1 is known to be a TGF-β activator, no antitumor effect was observed, at least at the same dose of anti-TSP1 mAb, suggesting that TSP1 would be a more potent effector molecule than TGF-β in the Snail-induced immunosuppressive mechanism (data not shown). Infiltration of immune cells, including CD4⁺ cells with reduced Foxp3, CD8⁺ cells with greater binding of gp70 tetramer, and I-A^{b+}CD11c⁺ DCs, was markedly increased in the anti-TSP1 mAb-injected tumors (Figure 6C). The amount of immune cells, particularly DCs, was more increased in these tumors, while the mAb efficacies to decrease Treg cells and expand tumor-specific CD8⁺ cells were inferior to those induced by *snail*-specific siRNA (Figure 5), implying the possibility that another molecule could be also involved in Snail-induced immunosuppression. However, these results indicate that TSP1 is one of the key mediators involved in Snail-induced immunosuppression. Further study will be required to identify the additional molecules involved.

It should be noted that i.t. injection with *snail*-specific siRNA or anti-TSP1 mAb more effectively inhibited growth of the mock transfectants with low Snail, and the treated tumors disappeared in some of these mice ($p < 0.0001$; Figure 5A; Figure 6A), following increased infiltration of immune cells such as CD4⁺ cells with low Foxp3, gp70 tetramer-binding CD8⁺ cells, and mature DCs, similar to our observations when *snail*-transduced tumor were injected i.t. (Figure 5C; Figure 6C). The survival of these mice was also significantly prolonged when observed over a longer term ($p < 0.0001$; 24 days for control mice versus 48 days for siRNA-*snail* mice and 34 days for anti-TSP1 mAb(+) mice). These data indicate that immunosuppression in vivo might also be caused by tumor cells with low levels of endogenous Snail expression.

Induction of CD4⁺Foxp3⁺ Cells by *snail*-Transduced Human Melanoma Cells with EMT-like Features

We then evaluated whether Snail-induced immunosuppression would be caused similarly by human melanoma. The human melanoma cell line HS294T transduced with the human *snail* gene showed typical EMT features such as spindle and dendritic

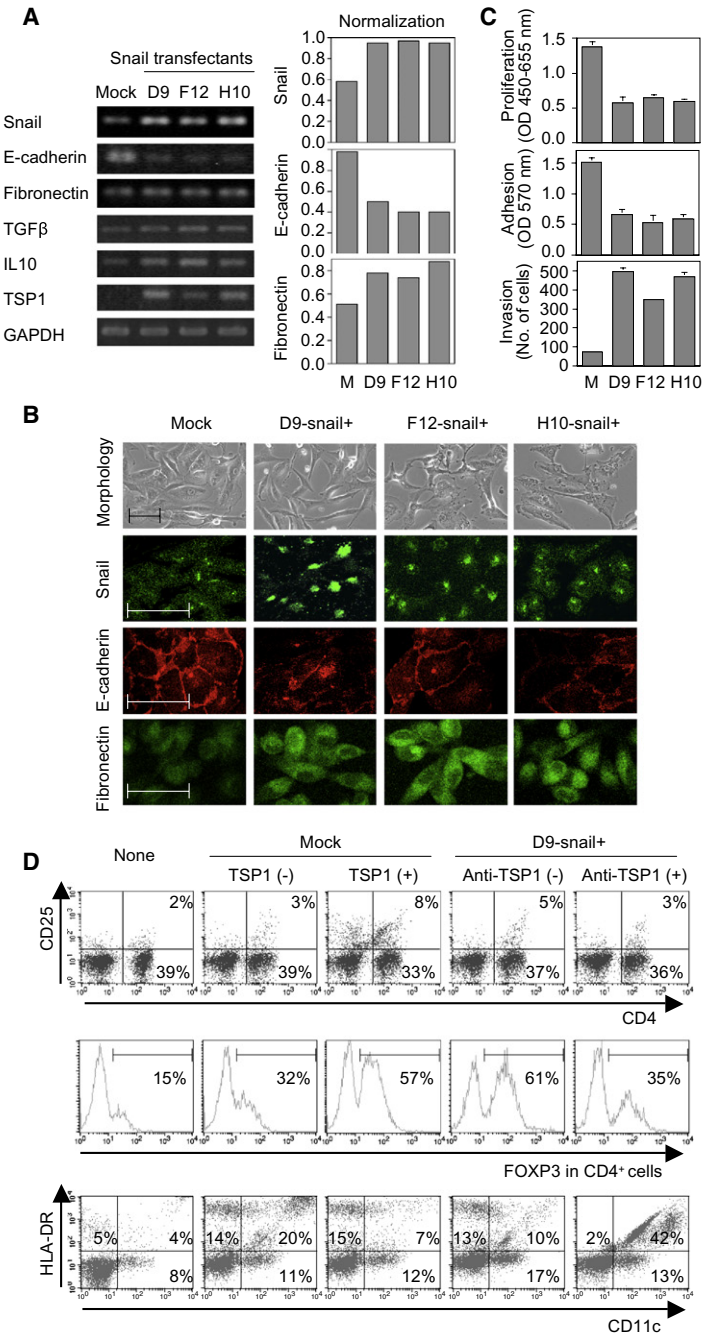

Figure 7. Immunosuppression Induced by *snail*-Transduced Human Melanoma HS294T Cells with EMT-like Characteristics

(A) Left: decrease of the epithelial marker *E-cadherin* and increase of the mesenchymal marker *fibronectin* and immunosuppressive cytokines (*TGF-β*, *IL10*, and *TSP1*) in the Snail transfectants detected by RT-PCR. Right: the intensity of *snail*, *E-cadherin*, and *fibronectin* was normalized to *GAPDH* expression as a control.

(B) Decrease of E-cadherin and increase of fibronectin in the Snail transfectants with spindle and dendritic shapes (immunocytochemistry; scale bars = 0.5 mm).

(C) EMT-like functional changes of Snail transfectants: decreased proliferation, decreased adhesion, and increased invasion (n = 3, mean ± SD).

(D) Increase of $CD4^+Foxp3^+$ cells and decrease of $CD11c^+HLA\text{-}DR^+$ cells induced by D9-snail+ tumor cells. Human peripheral blood mononuclear cells (PBMCs) were cocultured with tumor cells with or without TSP1 or anti-TSP1 mAb for 5 days. The percentage of each positive fraction was analyzed by flow cytometry.

Data shown in each panel are representative of two independent experiments.

shapes, decreased cell proliferation and adhesion, and increased cell invasion accompanied by decreased E-cadherin and increased fibronectin (Figures 7A–7C). Also, these transfectants showed increased mRNA expression of *TGF-β*, *IL-10*, and *TSP1*. When human peripheral blood mononuclear cells (PBMCs) were cocultured with one of the Snail transfectants, D9-snail+, $CD4^+CD25^+$ cells were slightly increased and FOXP3 expression in the $CD4^+$ cells was significantly increased ($p < 0.01$; Figure 7D; Table S1). $CD11c^+HLA\text{-}DR^+$ cells were less numerous as compared with those cocultured with the mock-transfected HS294T cells (Figure 7D). When TSP1 was added to the culture with mock-transfected tumor cells and PBMCs, Treg induction was increased and mature DC induction was inhibited (Figure 7D). Conversely, Treg induction was significantly decreased ($p < 0.014$; Table S1) and mature DC induction was markedly increased when anti-TSP1 mAb was added to the culture with D9-snail+ tumor cells and PBMCs (Figure 7D). These data also suggest TSP1 involvement in the immunosuppression induced by human $Snail^+$ melanoma. In addition, such immunosuppressive effects were similarly induced by other *snail*-transduced melanoma cell lines and other types of cancer cell lines such as pancreatic cancers or colon cancers (data not shown). These results indicate that human $Snail^+$ cancer cells induce immunosuppression as well as murine $Snail^+$ melanoma cells.

Induction of EMT and Immunosuppression by Endogenous Snail Is Increased by TGF-β Treatment in Human Melanoma Cells

We further examined the relationship between naturally occurring EMT in tumor cells and immunosuppression using various human melanoma cell lines. When human PBMCs were cocultured with melanoma cells with or without TGF-β, the level of $CD4^+Foxp3^+$ cell induction was correlated with *snail* expression induced by TGF-β (Figure 8A). Similar results were also observed in ARPE19 retinal pigment epithelial cells treated with TGF-β, suggesting that immunosuppression could also be caused by Snail-induced EMT even in noncancerous cells. $CD4^+FOXP3^+$ cells were not increased when cocultured with siRNA-*snail*(+) melanoma cells even after TGF-β treatment (Figure 8B), possibly because TSP1 production from melanoma cells was reduced at the same time that tumor invasion was suppressed by siRNA-*snail* transfection (Figure 8C), suggesting that the increased endogenous Snail could be correlated with induction of both EMT and immunosuppression in various human melanoma cells. These results indicate that the data obtained using *snail*-transduced melanoma cells reflect the naturally occurring, Snail-induced EMT.

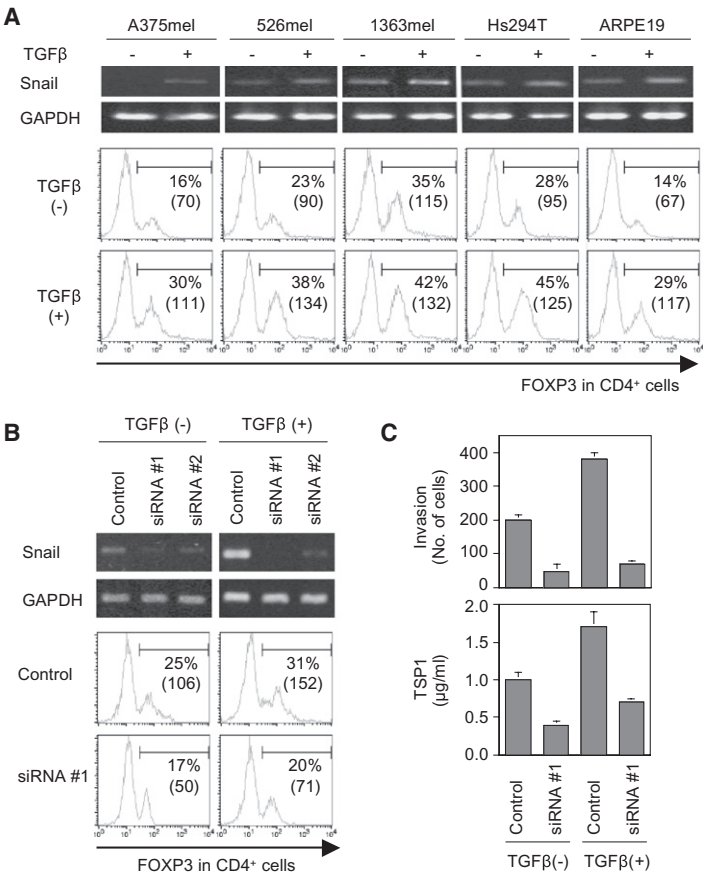

Figure 8. Induction of CD4$^+$Foxp3$^+$ Cells by Human Melanoma Cells with High Invasive Ability after TGF-β Treatment

(A) Increase of CD4$^+$Foxp3$^+$ cells in human PBMCs correlates with *snail* expression in human melanoma or normal cells cocultured together for 5 days.

(B) Inhibition of CD4$^+$Foxp3$^+$ cell induction by *snail* knockdown in HS294T melanoma cells after transfection with *snail*-specific siRNA. Top: *snail* mRNA expression analyzed by RT-PCR. Bottom: Foxp3 induction in CD4$^+$ cells analyzed by flow cytometry. The numbers in parentheses indicate the Foxp3 MFI of CD4$^+$Foxp3$^+$ cells.

(C) Inhibition of cell invasion and TSP1 production of HS294T melanoma cells by transfection with *snail*-specific siRNA (n = 3, mean ± SD). Melanoma cells or normal ARPE19 epithelial cells treated with TGF-β (5 ng/ml) for 3 days were used after washing for assays.

Data shown in each panel are representative of two independent experiments.

Taken together, our data demonstrate that Snail-associated EMT accelerates melanoma metastasis through not only enhanced invasive ability but also severe immunosuppression mediating induction of immunosuppressive cytokines and generation of Treg cells and impaired DCs. Therefore, *snail*-targeting therapy could simultaneously inhibit both cancer metastasis and immunosuppression including multiple suppressive molecules and/or cells in cancer patients.

DISCUSSION

EMT is thought to be a key step toward tumor metastasis via induction of highly invasive cancer cells, and its molecular mechanisms have been intensively studied. However, how cancer cells influence the host immune system during EMT is unclear. In this study, we demonstrate that Snail-induced EMT accelerates tumor metastasis via both enhanced invasive ability and immunosuppression. Snail$^+$ melanoma with typical EMT features severely induced immunosuppression both in vitro and in vivo. Notably, almost no infiltration of antitumor effector cells was observed in the local tumor sites in vivo, and almost no CD8$^+$ responses specific for tumor antigens were induced, resulting in enhanced tumor metastasis in various organs of the mice implanted s.c. with Snail$^+$ tumors. These events could possibly be mediated by induction of Treg cells with high Foxp3 expression and impaired DCs with low costimulatory molecule expression but high IDO expression, as observed in vitro.

Snail$^+$ melanoma cells appear to generate immunosuppressive nTreg-like CD4$^+$CD25$^-$ cells rather than to increase CD4$^+$CD25$^+$ nTreg cells, partly by mediating Treg-inducible cytokines such as TGF-β and TSP1. In addition to the direct effect of these cytokines, impaired DCs with low costimulatory molecule expression and high IDO (an immunosuppressive enzyme that acts via tryptophan deficiency) generated by Snail$^+$ melanoma cells are indirectly important for the induction of nTreg-like CD4$^-$CD25$^-$ cells in a cell-cell contact manner. TSP1 is thought to be one of the major factors involved in in vitro and in vivo immunosuppression; however, other immunosuppressive mechanisms may be also involved in the Snail-induced events, since the production level of the immunosuppressive factors appears to be different among various cancer cells.

This study reveals that Snail$^+$ melanoma is resistant to DC-based immunotherapy (CA/DC-IT), which is usually effective in suppressing Snail$^-$ B16-F10 melanoma followed by induction of antitumor immune responses. No antitumor T cell responses were induced in mice with Snail$^+$ melanoma even after the CA/DC-IT therapy because of Snail-induced immunosuppression mediated by nTreg-like CD4$^+$Foxp3$^+$ cells and impaired DCs. Additionally, Snail$^+$ melanoma itself was resistant to CTL lysis. EMT of tumor cells is reportedly associated with resistance to chemotherapeutics such as paclitaxel and gemcitabine (Kajiyama et al., 2007; Shah et al., 2007). We also observed resistance of our Snail transfectants to 5-fluorouracil, cyclophosphamide, and paclitaxel, as previously reported by others (data not shown). In this study, we demonstrate that Snail-induced EMT also renders melanoma cells resistant to CTL attack as well as to chemotherapeutics.

These findings obtained with the *snail*-transduced melanoma are applicable to the naturally occurring Snail-induced EMT. Both the invasive ability and the Treg-inducible ability of human melanoma cells are correlatively enhanced by endogenous Snail increase after TGF-β treatment, and both abilities were abrogated by *snail*-specific siRNA transfection (Figure 8). In addition, injection with *snail*-specific siRNA was also effective in inhibiting mock transfectants with low expression of endogenous Snail (Figure 5). Snail-induced immunosuppressive cascades would be applicable for patients with various cancers because such phenomena have been similarly induced by other human cancer

cell lines transduced with *snail*, including pancreatic cancers and colorectal cancers (data not shown). Thus, our study demonstrates that cancer EMT and immunosuppression can be simultaneously induced by Snail, which is predominantly involved in EMT induced by various stimuli in a variety of human cancers. However, it is not clear whether both are necessarily induced together or whether each event is induced separately. Further studies including analysis of EMT regulated by other transcription factors such as Slug and Twist are required.

Recently, many other studies have been reported involving a variety of immunosuppressive molecules such as TGF-β, IL-10, VEGF, and IL-6 and a variety of immunosuppressive cells such as $CD4^+$ Treg cells, $CD8^+$ Treg cells (Bisikirska et al., 2005; Rifa'i et al., 2004), natural killer T cells (Kronenberg and Rudensky, 2005), γδ cells (Koshiba et al., 2007), tumor-associated macrophages (Porta et al., 2007), and myeloid-derived suppressor cells (Talmadge, 2007). Correlation between increases in these suppressive factors and poor patient prognosis (Beyer and Schultze, 2006; Rouse, 2007; Waldmann, 2006) has been demonstrated. Based on recent progress in human tumor immunology, various active immunization trials have been attempted in cancer patients (Rosenberg et al., 2004). However, the efficacy of these trials has been limited so far. One of the major problems is thought to be systemic and local immunosuppression mediated by known and unknown mechanisms in cancer patients. The comprehensive inhibition of these multiple immunosuppression factors will be required for improvement of antitumor immune responses in cancer patients. In this study, *snail* knockdown in $Snail^+$ melanoma using *snail*-specific siRNA abrogated Snail-induced effects, both tumor metastasis and immunosuppression, followed by tumor inhibition along with local infiltration of antitumor effector cells in tumor tissues and systemic induction of tumor-specific $CD8^+$ T cell responses in vivo. Inhibition of the EMT upstream molecule Snail could be effective in simultaneously blocking both cancer invasion and immunosuppression. This strategy would be an attractive approach to improving the antitumor efficacies of a variety of cancer therapies.

EXPERIMENTAL PROCEDURES

Cell Lines and Mice

Murine melanoma cell line B16-F10; human melanoma cell lines HS294T, A375mel, 526mel, and 1363mel; and human retinal pigment epithelial cell line ARPE19 were used. Female C57BL/6 mice were purchased from SLC (Japan) and maintained under pathogen-free conditions until used for experiments. Mice were used upon approval by the Animal Care and Use Committee of Keio University School of Medicine. In some experiments, cells were treated with TGF-β, TNFα, or TSP1 (5 ng/ml) for 3 days to induce EMT.

snail Gene Transfection

Tumor cells were transfected with plasmid vector pcDNA3.1(+) (Invitrogen) encoding either murine or human *snail* cDNA or with the empty vector as mock transfection by electroporation (0.4 kV, 25 microfaradays) and selected with G418 in 10% FCS-containing DMEM. Cells were trypsinized and washed in PBS before use in assays.

RT-PCR

Each cDNA was synthesized with an oligo(dT) primer from total RNA extracted from cells using an RNeasy kit (QIAGEN) according to the manufacturer's instructions and was amplified with specific paired primers and Ex Taq polymerase (Takara) by PCR as follows: denaturation at 94°C for 30 s, 30 cycles of annealing at 55°C–65°C for 30 s, and elongation at 72°C for 60 s. The primers used for detection of murine and human gene expression are shown in Table S3. Digital images of the bands were analyzed and quantified using NIH ImageJ software (http://rsb.info.nih.gov/ij/), and each signal intensity was normalized to *GAPDH* expression as a control.

Immunocytochemistry

To analyze expression and localization of specific proteins in cells, tumor cells were prepared by culture in a slide chamber for 24 hr or by cytospin before staining. After treatment with Cytofix/Cytoperm solution (BD Pharmingen), tumor cells were stained with anti-Snail mAb (Santa Cruz Biotechnology), anti-E-cadherin mAb (BD Pharmingen), anti-fibronectin mAb (R&D Systems), or the appropriate isotype control antibodies. Alexa 488 (green)- or Alexa 568 (red)-conjugated secondary antibodies (Invitrogen) were used for visualization, and cells were observed using a confocal LSM 5 Pascal microscope (Carl Zeiss Meditec).

Functional Characterization of Tumor Cells

To evaluate cell adhesion, tumor cells (4×10^4 cells/well) were cultured in fibronectin-coated 96-well plates (BD Biosciences) for 1 hr at 37°C (n = 3). After vigorous vortexing for 30 s, the nonadherent cells were discarded and treated with a fixation/staining solution containing 0.5% crystal violet, 12% formaldehyde, and 10% ethanol for 15 min. After washing in water and then drying, 1% SDS solution (100 μl/well) was added, and the extract absorbance was measured at 570 nm. To evaluate cell invasion, 4×10^4 cells/well were cultured in 1% BSA/PBS in the upper compartment of a transwell chamber with a Matrigel-coated membrane (pore size = 8 μm; BD Biosciences) using 24-well plates for 16 hr at 37°C (n = 3). After scraping cells on the surface using cotton swabs, the membrane was treated with the fixation/staining solution, and the invaded cells were counted under a microscope. To evaluate cell proliferation, 2×10^4 cells/well were cultured in 96-well flat-bottom plates for 3 days at 37°C (n = 3), and WST-1 solution (Takara) was added into each well. After additional culture for 3–4 hr, absorbance was measured at 450–655 nm. Cytokine production from tumor cells (3-day culture) was measured using ELISA kits (TGF-β and IL-10, R&D Systems; TSP1, Chemicon) according to the manufacturers' instructions. To evaluate in vivo tumor growth, 1×10^6 tumor cells were implanted s.c. into the right flank of C57BL/6 mice. Tumor size was measured 1–2 times per week, and the volume in mm^3 was calculated as follows: $0.5 \times \text{length} \times \text{width}^2$. To evaluate the in vivo metastatic ability of tumor cells and mouse survival after tumor implantation, 2×10^5 tumor cells were injected i.v. in the tail vein of mice.

In Vitro Stimulation of Immune Cells with Tumor Cells

In the murine system, spleens were pooled and dispersed into single-cell suspensions, and SPCs were isolated by Ficoll-Paque (Amersham) followed by treatment with ACK solution (BioWhittaker). 1×10^6 SPCs were stimulated with 1×10^5 irradiated or mitomycin C (MMC)-treated tumor cells in 10% FCS-containing RPMI1640 (37°C, 5% CO_2) for 5 days. In some experiments, SPCs were separated into specific cell populations ($CD4^+$ or $CD11c^+$) utilizing a magnetic-activated cell sorting separation system with mAb-conjugated MicroBeads according to the manufacturer's instructions (Miltenyi Biotec) and/or separately cultured using a transwell chamber with a membrane (pore size = 0.4 μm; Cell Culture Insert, Becton Dickinson). For DC analysis, 1×10^6 BMCs from femurs after Ficoll isolation were separated into $CD11c^+$ cells using anti-CD11c mAb-conjugated MicroBeads, and the $CD11c^+$ cells were cultured with GM-CSF (10 ng/ml, PeproTech) and/or irradiated tumor cells (10:1) for 6 days. To evaluate TSP1 effects on DCs, the purified $CD11c^+$ cells were stimulated with TSP1 (0.5 μg/ml, R&D Systems) for 5 days. To block IDO induction in the DCs, the IDO inhibitor 1-methyltryptophan (1MT, Sigma) was added at 1 mM to the culture. Anti-TSP1 (Calbiochem), anti-CD36 (Abcam), or anti-CD47 mAb (BD Pharmingen) was added to the culture to examine the involvement of these receptors in the TSP1-induced mechanism.

In the human system, human peripheral blood cells from healthy volunteers were also isolated by Ficoll-Paque followed by treatment with ACK solution. The mononuclear cells (PBMCs) at the interface between blood and Ficoll-Paque solution were harvested, and these PBMCs (1×10^6 cells) were stimulated with 1×10^5 irradiated or MMC-treated tumor cells or the supernatant (3-day culture, 2× dilution) at 37°C for 5 days. For DC analysis,

1×10^6 $CD14^+$ cells separated from PBMCs using anti-CD14 mAb-conjugated MicroBeads were cultured with irradiated tumor cells (10:1) for 5 days. To block the specific cytokine in the culture, mAbs specific for TGF-β (R&D Systems), IL-10 (R&D Systems), or TSP1 (Calbiochem) were added at 2–5 μg/ml.

Flow Cytometric Analysis

To examine tumor cell effects on immune cells in vitro and in vivo, specific markers were analyzed by flow cytometry. Fc receptor was blocked by anti-CD16/CD32 mAb before immunofluorescence staining. The following antibodies conjugated with FITC, phycoerythrin, or CyChrome were used for analysis: anti-Foxp3, anti-CD4, anti-CD25, anti-CTLA4, anti-HO-1, anti-granzyme B, anti-PD1, anti-CD8, anti-CD11c, anti-$I\text{-}A^b$, anti-CD80, anti-IDO, anti-HLA-DR, or the appropriate isotype-matched control antibodies. Antibodies and isotype controls were purchased from BD Pharmingen, except anti-Foxp3 mAb (eBioscience), anti-HO-1 (Abcam), anti-granzyme B (eBioscience), and anti-IDO mAb (Serotec). For intracellular staining of Foxp3, CTLA-4, HO-1, granzyme B, and IDO, cells were treated with Cytofix/Cytoperm solution (BD Pharmingen) according to the manufacturer's instructions. The immunofluorescence was compared to the appropriate isotype controls and analyzed with CellQuest software using a FACSCalibur cytometer (Becton Dickinson).

Immunosuppressive Activity of $CD4^+$ Cells and DCs

To evaluate the immunosuppressive activity of $CD4^+$ cells stimulated with tumor cells, $CD4^+$ cells were separated from the cultured spleen cells after stimulation with Snail transfectants for 5 days. The prestimulated $CD4^+$ cells were added to the culture with fresh and purified splenic $CD4^+$ or $CD8^+$ cells at a 1:1 ratio in addition to APCs (irradiated bulk SPCs) and anti-CD3 mAb (1 μg/ml) for 5 days (n = 3). To evaluate APC function of the BMC-derived $CD11c^+$ cells stimulated with tumor cells, the precultured $CD11c^+$ cells were added to fresh and purified splenic $CD4^+$ or $CD8^+$ cells (1:1) and cultured with anti-CD3 mAb (1 μg/ml) for 5 days (n = 3). Cell proliferation was evaluated by WST-1 assay.

RNA Interference Assay In Vitro and In Vivo

For *snail* knockdown in tumor cells, FITC-conjugated siRNAs (Invitrogen) specific for murine or human *snail* were used in assays in vitro and in vivo after the optimal transfection condition was determined initially. FITC-labeled siRNA-*snail* or scrambled oligonucleotide control (Invitrogen) was diluted in 150 mM NaCl and mixed with 7.5 mM jetPEI (Polyplus Transfection), a cationic polymer transfection reagent useful for gene delivery in vitro and in vivo (Urban-Klein et al., 2005). The complexes were incubated for 15 min and then added to cells at 50%–60% confluence. Typically, 3×10^5 tumor cells were seeded in six-well plates, 2 μg jetPEI/siRNA-*snail* was added 24 hr later, and the cells used for assays within 2–6 days after transfection. The transfection efficacy was validated by flow cytometry before use; >80%–90% of the cells were FITC positive. *snail* expression was evaluated by RT-PCR and immunocytochemistry. For *snail* knockdown in vivo, jetPEI/siRNA-*snail* (3 μg) was injected i.t. on day 7 after tumor implantation. The transfection efficacy was validated by flow cytometry 1–2 days after injection; >60%–70% of the cells were FITC positive in cells harvested from the injected tumors. *snail* expression in the tumor sites was evaluated by RT-PCR using Ampdirect Plus (Shimadzu) according to the manufacturer's instructions.

Tumor Therapy In Vivo

C57BL/6 mice were implanted s.c. with B16-F10 tumor cells into the right flank (1×10^6 cells/site) and received the following combination immunotherapy on day 7 after tumor implantation (n = 5–7): tumors were cryoablated at −80°C for 60 s using a Keeler Cryomaster and then directly injected with DCs (2×10^6 cells/mouse), which were pulsed with the $H\text{-}2K^b$-restricted peptide $p15E_{604–611}$ (1 μg/ml, KSPWFTTL, referred as gp70 peptide) for 6 hr before use. In the experiments using TGF-β-treated tumor cells, to evaluate the antitumor effect on tumor metastasis, mice were implanted both s.c. at the right flank (1×10^6 cells) and i.v. in the tail vein (2×10^5 cells) and then received the same immunotherapy on day 5 after tumor implantation (n = 3–5). In the experiments to evaluate TSP1 blockade effect in vivo, tumors were directly injected with anti-TSP1 mAb (50 μg/mouse) on day 7 after tumor implantation (n = 3). Mice were sacrificed on day 14, and tumors and other tissues (peripheral blood, bone marrow, spleens, inguinal lymph nodes, and lungs) were harvested and mechanically dispersed into single-cell suspensions for assays (n = 3–5, pooled). To examine tumor micrometastasis in organs after s.c. tumor implantation, RT-PCR for the melanoma antigen *gp100* was conducted using specific primers with Ampdirect Plus.

Evaluation of Tumor-Specific $CD8^+$ T Cell Responses

To evaluate $CD8^+$ T cell immune responses specific for tumor antigens, as described previously (Kudo-Saito et al., 2005), SPCs were first stimulated with 1 μg/ml of gp70 peptide or the $H\text{-}2D^b$-restricted peptide $gp100_{25–33}$ (KVPRNQDWL). Six days later, bulk lymphocytes were separated by Ficoll-Hypaque isolation, and the recovered $CD8^+$ T cells were tested for cytokine production and tumor-killing activity. In cytokine production assay, 5×10^5 recovered $CD8^+$ T cells were restimulated with 5×10^6 fresh irradiated naive splenocytes as APCs and 1 μg/ml peptide for 24 hr (n = 3), and the supernatant fluid was analyzed for IFN-γ using a Cytometric Bead Array kit (BD Pharmingen). A small amount of IFN-γ (less than 20 pg/ml) was detected in each SPC culture supernatant with the control peptide ($H\text{-}2K^b$-restricted β-galactosidase$_{96–103}$, 1 μg/ml, DAPIYTNV) or no peptide (spontaneous production). In cytotoxicity assay using an annexin V system (Immunocyto Cytotoxicity Detection Kit, MBL), 1×10^5 target tumor cells were incubated with the recovered $CD8^+$ T cells for 4 hr (n = 3) and analyzed by flow cytometry according to the manufacturer's instructions.

Statistical Analysis

Significant differences ($p < 0.05$) were evaluated using the unpaired two-tailed Student's t test. For graphical representation of data, y axis error bars indicate the standard deviation of the data for each point on the graph. Mouse survival was evaluated by the Kaplan-Meier method and ranked according to the Mantel-Cox log-rank test.

SUPPLEMENTAL DATA

The Supplemental Data include three tables and four figures and can be found with this article online at http://www.cancercell.org/supplemental/S1535-6108(09)00032-4.

ACKNOWLEDGMENTS

This work was supported by Grants-in-Aid for Scientific Research 18591484, 19390355, and 17016070 from the Japanese Ministry of Education, Culture, Sports, Science and Technology; the Uehara Memorial Foundation; and the Yasuda Medical Foundation.

Received: May 1, 2008
Revised: September 17, 2008
Accepted: January 23, 2009
Published: March 2, 2009

REFERENCES

Becker, K.F., Rosivatz, E., Blechschmidt, K., Kremmer, E., Sarbia, M., and Hofler, H. (2007). Analysis of the E-cadherin repressor Snail in primary human cancers. Cells Tissues Organs *185*, 204–212.

Beyer, M., and Schultze, J.L. (2006). Regulatory T cells in cancer. Blood *108*, 804–811.

Bisikirska, B., Colgan, J., Luban, J., Bluestone, J.A., and Herold, K.C. (2005). TCR stimulation with modified anti-CD3 mAb expands CD8+ T cell population and induces CD8+CD25+ Tregs. J. Clin. Invest. *115*, 2904–2913.

Crawford, S.E., Stellmach, V., Murphy-Ullrich, J.E., Ribeiro, S.M., Lawler, J., Hynes, R.O., Boivin, G.P., and Bouck, N. (1998). Thrombospondin-1 is a major activator of TGF-β1 in vivo. Cell *93*, 1159–1170.

Dissanayake, S.K., Wade, M., Johnson, C.E., O'Connell, M.P., Leotlela, P.D., French, A.D., Shah, K.V., Hewitt, K.J., Rosenthal, D.T., Indig, F.E., et al. (2007). The Wnt5A/protein kinase C pathway mediates motility in melanoma cells via

the inhibition of metastasis suppressors and initiation of an epithelial to mesenchymal transition. J. Biol. Chem. *282*, 17259–17271.

Doyen, V., Rubio, M., Braun, D., Nakajima, T., Abe, J., Saito, H., Delespesse, G., and Sarfati, M. (2003). Thrombospondin 1 is an autocrine negative regulator of human dendritic cell activation. J. Exp. Med. *198*, 1277–1283.

Futagami, Y., Sugita, S., Vega, J., Ishida, K., Takase, H., Maruyama, K., Aburatani, H., and Mochizuki, M. (2007). Role of thrombospondin-1 in T cell response to ocular pigment epithelial cells. J. Immunol. *178*, 6994–7005.

Hay, E.D. (1995). An overview of epithelio-mesenchymal transformation. Acta Anat. (Basel) *154*, 8–20.

Herlyn, M., Berking, C., Li, G., and Satyamoorthy, K. (2000). Lessons from melanocyte development for understanding the biological events in naevus and melanoma formation. Melanoma Res. *10*, 303–312.

Huber, M.A., Kraut, N., and Beug, H. (2005). Molecular requirements for epithelial-mesenchymal transition during tumor progression. Curr. Opin. Cell Biol. *17*, 548–558.

Hugo, H., Ackland, M.L., Blick, T., Lawrence, M.G., Clements, J.A., Williams, E.D., and Thompson, E.W. (2007). Epithelial-mesenchymal and mesenchymal-epithelial transitions in carcinoma progression. J. Cell. Physiol. *213*, 374–383.

Kajiyama, H., Shibata, K., Terauchi, M., Yamashita, M., Ino, K., Nawa, A., and Kikkawa, F. (2007). Chemoresistance to paclitaxel induces epithelial-mesenchymal transition and enhances metastatic potential for epithelial ovarian carcinoma cells. Int. J. Oncol. *31*, 277–283.

Koshiba, T., Li, Y., Takemura, M., Wu, Y., Sakaguchi, S., Minato, N., Wood, K.J., Haga, H., Ueda, M., and Uemoto, S. (2007). Clinical, immunological, and pathological aspects of operational tolerance after pediatric living-donor liver transplantation. Transpl. Immunol. *17*, 94–97.

Kronenberg, M., and Rudensky, A. (2005). Regulation of immunity by self-reactive T cells. Nature *435*, 598–604.

Kudo-Saito, C., Schlom, J., Camphausen, K., Coleman, C.N., and Hodge, J.W. (2005). The requirement of multimodal therapy (vaccine, local tumor radiation, and reduction of suppressor cells) to eliminate established tumors. Clin. Cancer Res. *11*, 4533–4544.

Kuphal, S., Palm, H.G., Poser, I., and Bosserhoff, A.K. (2005). Snail-regulated genes in malignant melanoma. Melanoma Res. *15*, 305–313.

Moody, S.E., Perez, D., Pan, T.C., Sarkisian, C.J., Portocarrero, C.P., Sterner, C.J., Notorfrancesco, K.L., Cardiff, R.D., and Chodosh, L.A. (2005). The transcriptional repressor Snail promotes mammary tumor recurrence. Cancer Cell *8*, 197–209.

Peinado, H., Quintanilla, M., and Cano, A. (2003). Transforming growth factor β-1 induces snail transcription factor in epithelial cell lines: mechanisms for epithelial mesenchymal transitions. J. Biol. Chem. *278*, 21113–21123.

Porta, C., Subhra Kumar, B., Larghi, P., Rubino, L., Mancino, A., and Sica, A. (2007). Tumor promotion by tumor-associated macrophages. Adv. Exp. Med. Biol. *604*, 67–86.

Radisky, D.C. (2005). Epithelial-mesenchymal transition. J. Cell Sci. *118*, 4325–4326.

Rifa'i, M., Kawamoto, Y., Nakashima, I., and Suzuki, H. (2004). Essential roles of CD8+CD122+ regulatory T cells in the maintenance of T cell homeostasis. J. Exp. Med. *200*, 1123–1134.

Rosenberg, S.A., Yang, J.C., and Restifo, N.P. (2004). Cancer immunotherapy: moving beyond current vaccines. Nat. Med. *10*, 909–915.

Rouse, B.T. (2007). Regulatory T cells in health and disease. J. Intern. Med. *262*, 78–95.

Shah, A.N., Summy, J.M., Zhang, J., Park, S.I., Parikh, N.U., and Gallick, G.E. (2007). Development and characterization of gemcitabine-resistant pancreatic tumor cells. Ann. Surg. Oncol. *14*, 3629–3637.

Sugimachi, K., Tanaka, S., Kameyama, T., Taguchi, K., Aishima, S., Shimada, M., Sugimachi, K., and Tsuneyoshi, M. (2003). Transcriptional repressor snail and progression of human hepatocellular carcinoma. Clin. Cancer Res. *9*, 2657–2664.

Talmadge, J.E. (2007). Pathways mediating the expansion and immunosuppressive activity of myeloid-derived suppressor cells and their relevance to cancer therapy. Clin. Cancer Res. *13*, 5243–5248.

Urban-Klein, B., Werth, S., Abuharbeid, S., Czubayko, F., and Aigner, A. (2005). RNAi-mediated gene-targeting through systemic application of polyethylenimine (PEI)-complexed siRNA in vivo. Gene Ther. *12*, 461–466.

von Boehmer, H. (2005). Mechanisms of suppression by suppressor T cells. Nat. Immunol. *6*, 338–344.

Waldmann, T.A. (2006). Effective cancer therapy through immunomodulation. Annu. Rev. Med. *57*, 65–81.

Yang, A.D., Camp, E.R., Fan, F., Shen, L., Gray, M.J., Liu, W., Somcio, R., Bauer, T.W., Wu, Y., Hicklin, D.J., et al. (2006). Vascular endothelial growth factor receptor-1 activation mediates epithelial to mesenchymal transition in human pancreatic carcinoma cells. Cancer Res. *66*, 46–51.

Yang, M.H., Chang, S.Y., Chiou, S.H., Liu, C.J., Chi, C.W., Chen, P.M., Teng, S.C., and Wu, K.J. (2007). Overexpression of NBS1 induces epithelial-mesenchymal transition and co-expression of NBS1 and Snail predicts metastasis of head and neck cancer. Oncogene *26*, 1459–1467.